available at www.sciencedirect.com

ScienceDirect

journal homepage: www.ejconline.com

# Treating triple-negative breast cancer by a combination of rapamycin and cyclophosphamide: An *in vivo* bioluminescence imaging study

*Qing Zeng* [a], *Zhong Yang* [b], *Yong-Jing Gao* [b], *Huaiping Yuan* [a], *Kemi Cui* [c], *Ying Shi* [a], *Hongyun Wang* [d], *Xudong Huang* [a], *Stephen T.C. Wong* [c], *Yaming Wang* [b], *Santosh Kesari* [e], *Ru-Rong Ji* [b], *Xiaoyin Xu* [a,*]

[a] *Department of Radiology, Brigham and Women's Hospital, Boston, MA, USA*
[b] *Department of Anaesthesia, Brigham and Women's Hospital, Boston, MA, USA*
[c] *Center for Biotechnology and Informatics, The Methodist Hospital Research Institute and Department of Radiology and Pathology, The Methodist Hospital, Weill Cornell Medical College, Houston, TX, USA*
[d] *Department of Medicine, Beth Israel Deaconess Medical Center, Boston, MA, USA*
[e] *Department of Neurosciences, Moores Cancer Center, University of California, San Diego, La Jolla, CA, USA*

ARTICLE INFO

*Article history:*
Received 5 October 2009
Received in revised form 5 January 2010
Accepted 14 January 2010
Available online 13 February 2010

*Keywords:*
Triple-negative breast cancer
Breast cancer metastasis
*in vivo* bioluminescence imaging
Rapamycin
mTOR
Cyclophosphamide
HIF-1α

ABSTRACT

Rapamycin, a mammalian target of rapamycin (mTOR) inhibitor, has been shown to inhibit the growth of oestrogen positive breast cancer. However, triple-negative (TN) breast cancer is resistant to rapamycin treatment *in vitro*. We set to test a combination treatment of rapamycin with DNA-damage agent, cyclophosphamide, in a TN breast cancer model. By binding to and disrupting cellular DNA, cyclophosphamide kills cells via interfering with their normal functions. We assessed the responses of nude mice bearing tumour xenografts of TN MDA-MB-231 cells to the combination of rapamycin and cyclophosphamide in both orthotopic mammary and lung-metastasis models. We tracked tumour growth and metastasis by bioluminescent imaging and examined the expression of Ki67, CD34 and HIF-1α in tumour tissues by immunohistochemistry and apoptosis index with TUNEL assay, and found that MDA-MB-231 cells are sensitive to rapamycin therapy in orthotopic mammary, but not in lung with metastasis. Rapamycin when combined with cyclophosphamide is found to have a more significant effect in reducing tumour volume and metastasis with a much improved survival rate. Our data also show that the sensitivity of TN tumours to rapamycin is associated with the microenvironment of the tumour cells. The data indicate that in a relatively hypoxic environment HIF-1α may play a role in mediating the anti-cancer effect of rapamycin and cyclophosphamide may prevent the feedback activation of Akt by rapamycin. Overall our results show that rapamycin plus cyclophosphamide can achieve an improved efficacy in suppressing tumour growth and metastasis, suggesting that the combination therapy can be a promising treatment option for TN cancer.



* *Corresponding author:* Address: Department of Radiology, Brigham and Women's Hospital, 221 Longwood Avenue, #013, Boston, MA 02115, USA. Tel.: +1 617 525 9596; fax: +1 617 278 6961.
E-mail address: xxu@bwh.harvard.edu (X. Xu).
0959-8049/$ - see front matter 
doi:10.1016/j.ejca.2010.01.014

## 1. Introduction

Triple-negative (TN) breast cancer, which is ER-negative, PR-negative and HER2 overexpression-negative, relapses quickly in response to clinical treatment[1] as this subtype of breast cancer has a high histological grade and a poor prognosis.[2] Patients with TN breast cancer, accounting for about 10–17% of all breast cancer cases,[3] are often unresponsive to endocrine agents such as trastuzumab and less responsive to standard adjuvant therapy.[4] Metastasis of TN breast cancer is often aggressive[1] and currently there is no recommended chemotherapy for the patients.[5] Some of the promising treatment regimens may consist of chemotherapy drugs and inhibitors of the mammalian target of rapamycin (mTOR) since the mTOR pathway is downstream of proto-oncogenes like Ras, PI3K, Akt, Rheb, eIF4E and Cyclin D1 as well as tumour suppressor genes such as PTEN, TSC1/2 and p53.[6]

Aberrant activation of the PI3K/Akt/mTOR pathway is involved in the oncogenesis and progression of breast cancer.[7] mTOR inhibitors, rapamycin and its analogs such as CCI-779, RAD001 and AP23573 have been introduced into clinical trials as anti-cancer agents. These agents generally have shown well-tolerable safety profiles and a promising anti-tumour effect in several types of refractory tumours.[8–10] However, clinical trials have shown only modest responses in 7–30% of cancer patients.[11] *In vitro* study shows that the TN MDA-MB-231 cells are resistant to growth inhibition induced by rapamycin.[12] Thomas and colleagues demonstrated that factors like HIF-1α level determine the sensitivity of kidney cancer cells to inhibition of mTOR (CCI-779).[13]

Several research findings suggest that the combination of rapamycin, a cytostatic agent, with DNA-damage agents could be optimal for solid tumour therapy. It has been shown that rapamycin can enhance carboplatin-induced cytotoxicity in HER2-overexpressing breast cancer cells[14] and mTOR inhibitor RAD001 can enhance the effect of cisplatin-induced apoptosis through inhibition of p21 translation.[15] Cyclophosphamide, an alkylating agent widely used in breast cancer therapy, causes DNA adducts, strand breaks and crosslink by binding to nucleophilic sites.[16] A combination of RAD001 with cyclophosphamide has shown synergistic anti-tumour activity in a gastric cancer mouse model.[17]

In this study we aim to determine whether a combination of rapamycin and cyclophosphamide has a potential improved anti-tumour effect on TN breast cancer cells (MDA-MB231) and whether the microenvironment of tumour growth has an impact on the sensitivity and resistance of TN tumour cells to mono- or combination therapy of rapamycin through HIF-1α. We first developed mouse xenograft tumour with luciferase-labelled cell line MDA-MB-231 as a preclinical TN breast cancer model and then investigated the response of the TN breast cancer to both therapeutic strategies *in vivo* via bioluminescence imaging and immunohistochemistry.

## 2. Materials and methods

### 2.1. Animal models

Female nude mice at the age of 6–8 weeks were purchased (Harlan Laboratory) and housed under standard conditions, fed with standard pelleted rodent chow and kept in a 12-h light/12-h dark cycle. All experimental procedures involving animals were approved by the institutional IRB. Prior to all surgical procedures, the animals were anesthetised with ketamine (100 mg/kg) and xylazine (15 mg/kg), according to the approved animal experiment protocol.

MDA-MB-231-luc-D3H2LN cell line stably expressing firefly luciferase was purchased from Caliper Life Sciences (Hopkinton, MA). The cells were cultured in Eagle's Minimum Essential Medium (ATCC, containing non-essential amino acids, 2 mM L-glutamine, 1 mM sodium pyruvate and 1500 mg/l sodium bicarbonate) supplemented with 10% fetal bovine serum (FBS), 1% penicillin-streptomycin and grown in a 5% $CO_2$ incubator at 37 °C before use. Orthotopic breast tumours were established by injecting $2 \times 10^6$ MDA-MB-231 cells (in 100 μl of PBS) into the fat pad of mouse mammary glands. Tumour volume was monitored weekly by measuring two perpendicular tumour diameters with a caliper and was calculated by the formula: tumour volume [$mm^3$] = (length [mm]) × (width [mm])$^2$ × 0.52. A lung-metastasis breast cancer model was established by injecting $1 \times 10^5$ MDA-MB-231 cells (in 100 μl of PBS) via tail veins of the mice. Mouse body weight was recorded weekly.

### 2.2. Drug preparation and treatment

Rapamycin was purchased from LC Laboratories (Woburn, MA). It was dissolved in DMSO (100 mg/ml) and was kept at −20 °C. Store solution was diluted with 1 × PBS to 1 mg/ml before use. Cyclophosphamide (Cytoxan®, Bristol-Myers Squibb Company) was directly dissolved in 1 × PBS (30 mg/ml). Both the working solutions were kept at 4 °C.

After implantation into the mice, the tumour cells were allowed to grow for 3 d without any treatment. Mice with orthotopic breast tumours were randomly divided into six groups: (1) vehicle (1% DMSO in PBS) group (control), (2) high-dose rapamycin-only group (Hi-Rapa), (3) low-dose rapamycin-only group (Lo-Rapa), (4) cyclophosphamide-only group (Cyclo), (5) combination group 1 (Hi-Rapa + Cyclo) and (6) combination group 2 (Lo-Rapa + Cyclo). There were 6–11 mice per group. For Hi-Rapa, Lo-Rapa and Hi- and Lo-Rapa + Cyclo groups, rapamycin treatment was administrated intraperitoneally (i.p.) at 5 mg/kg for the high-dose group and 1.5 mg/kg for the low-dose group. Rapamycin was given for 6 consecutive days, stopped for 1 d and then repeated for four cycles. For Cyclo and Rapa + Cyclo groups, cyclophosphamide was given by i.p. at 150 mg/kg on day 1, 3, 5, followed by a 2-week break, and the above-mentioned procedure was repeated. The mice were treated for 4 weeks in total. For the mice that were implanted with tumour cells via tail vein injection, they were randomly divided into four groups: (1) control group, (2) Hi-Rapa group, (3) Cyclo group and (4) Hi-Rapa + Cyclo group. There were five mice per group. Drug treatment regimen was the same as described above for orthotopic tumour-bearing mice, but lasted for 8–14 weeks. At the end of the experiments, we harvested the tumour samples for histology.

### 2.3. Cell cytotoxicity assay

Cytotoxicity tests were performed using the Promega CellTiter 96 Aqueous Non-Radioactive Cell Proliferation (MTS) assay to

determine the viability of the cells in culture (Promega, G3582, USA). Monolayers of 5000 MDA-MB-231 cells were plated into a flat-bottomed 96-well cell culture plates (Corning Incorporated, USA) in Minimum Essential Medium (ATCC, 30-2003) containing 10% fetal bovine serum (FBS). At 24 h after plating, when the cells had attached and reached above 50% confluence, the medium was replaced with another medium including various concentrations of drugs. All the experiments were performed for 48 h and in triplicates. Controls included 0.001% DMSO. Rapamycin was used at concentrations of 10, 50 and 100 nM and cyclophosphamide at 1, 5 and 10 mM. Each experiment was reproduced and confirmed in three independent experiments. After treatment, one solution reagent at 20 μl per well was added directly to the culture wells. After incubating for 3 h, the plate was read by microplate spectrophotometer. The absorbance of the formazan product was at 490 nm.

### 2.4. Bioluminescent Imaging

Mice were anesthetised with a mixture of oxygen and 1.5% of isoflurane (Webster Veterinarian, Sterling, MA) before imaging. The substrate luciferin, D-Luciferin (Caliper Life Sciences, Hopkinton, MA) in PBS (15 mg/ml) was injected intraperitoneally at a dose of 75 mg/kg of body weight. The mice were imaged by the IVIS 100 system (Xenogen, Alameda, CA), and the bioluminescence signals were quantified by the Living Image® software. We acquired images every 5 min until 5–10 min after recording the maximum reading. A typical exposure time was 10–30 s for orthotopic xenograft mice and 1–3 min for lung-metastasis mice. Binning number was set to medium and FOV was set to level D. We performed analyses of the images by drawing a region of interest (ROI) over the tumour to obtain the normalised photons per second over the ROIs.

### 2.5. Immunohistochemistry

Tumour samples were obtained from MDA-MB-231 orthotopic and lung-metastatic breast cancer in the mouse models. Immunofluorescence staining of Ki67, a proliferation marker, was performed on 10 μm thick frozen sections of MDA-MB-231 tumour. The sections were blocked with 5% normal goat serum +2% BSA +0.2% TritonX-100 in PBS at room temperature for 2 h, reacted with primary antibody ki67 (1:800, Abcam) at 4 °C overnight. Then the sections were treated with a second antibody Cy3-goat-anti-rabbit (1:400, Jackson) at room temperature for 1 h and counterstained with DAPI (1:2000, Sigma). Using a 10× objective, three to four digital images were captured with Advanced Spot Software (Digital Camera System, Diagonostic Instruments) from 3 to 4 breast tumour segments for each animal. In each image, the ratio of the number of $Ki67^+$ cells versus the total number of nuclei in tumour ($Ki67^+$ cells/$DIPA^+$ cells) was calculated by using the ImageJ software (NIH) in terms of proliferation index.

The levels of CD34 and HIF-1α were determined by immunohistochemistry. Paraffin-embedded sections were deparaffinised and rehydrated. CD34 slides were retrieved with citrate (pH 6, Zymed, South San Francisco, CA), and HIF-1α slides were retrieved by EDTA (pH 8, Zymed) in a steam pressure cooker for 2 min. The sections were pretreated with 0.3% $H_2O_2$ block for 5–10 min to quench endo-peroxidase activity. Then, the sections were exposed overnight at 4 °C to 200 μl of specific antibodies against mouse CD34 (Abcam, 1:100 diluted in DAKO Ab diluents, Zymed) or human HIF-1α (Neo-Mark, UK, 1:2000 with a tyramide application kit). We used the second antibody of rabbit anti-rat (1:750, DAKO) for CD34 staining and envision anti-mouse (1:500, DAKO) for HIF-1α slides according to the manufacturer's instructions. After further wash, immunoperoxidase staining was developed using a DAB chromogen (DAKO) and counterstained with hematoxylin for 4 s. The slides were examined under a 4× objective of a microscope. We first identified three hot spots of positive area and then photographed them at 10× amplification. A single endothelial cell or a cluster of endothelial cells positive for CD34 was considered as a vessel. The number of microvessels in a histological field was counted as microvessel density (MVD).[18] Similarly, the number of HIF-1α positive with nuclei per field was defined as the HIF-1α score.

### 2.6. TUNEL assay

Apoptosis was determined by TUNEL assay using TdT and Biotin-16-dUTP purchased from Roche Diagnostic (Indianapolis, IN). We used paraffin sections of orthotic samples and frozen lung-metastasis samples for TUNEL staining. Paraffin sections were pretreated with proteinase K for 15 min and sodium borohydride (1 mg/ml) for 10 min, and the frozen sections was treated with sodium borohydride only. The sections were pre-incubated in TdT Reaction Buffer for 10 min, followed by incubation with TdT Reaction Mixture for 1 h at 37 °C in a humidified chamber. The reaction was terminated with stop wash buffer (30 mmol/l of NaCl and 3 mmol/l of sodium citrate, pH 7.2, rinse for 10 min). HRP-avidin (30 min) and DAB development (3–8 min) were used in the paraffin section, and the frozen sections were incubated with Cy5-conjugated avidin in TBS (1:200) for 30 min at room temperature. Nuclear counterstaining was performed with hematoxylin or DAPI. Apoptotic bodies in the tumour sections of each sample were quantified by counting the number of TUNEL-positive cells in three randomly selected, non-overlapping regions using an inverted Nikon TE300 microscope.

### 2.7. Western blots

MDA-MB-231 cells ($4 \times 10^4$) were plated and grown in 12-well culture plate for 24 h. The cells were treated with 100 nM rapamycin, 5 mM cyclophosphamide and Rapa-Cyclo combination for 6, 24, 48 and 72 h. After washing with cold PBS, the cells were subjected to lysis using RIPA lysis buffer (Thermo #89901, USA) plus protein inhibitors according to the manufacturer's instructions. Same amount of protein lysate was loaded into NuPAGE 4–12% Tris–Bis gel (Invitrogen, USA) and then electrotransferred to nitrocellose membrane. The membranes were blocked with TBST (0.1% Tween 20) containing 5% BSA for pAkt and 5% non-fat dry milk for Akt antibody for 1 h at room temperature and incubated with different primary

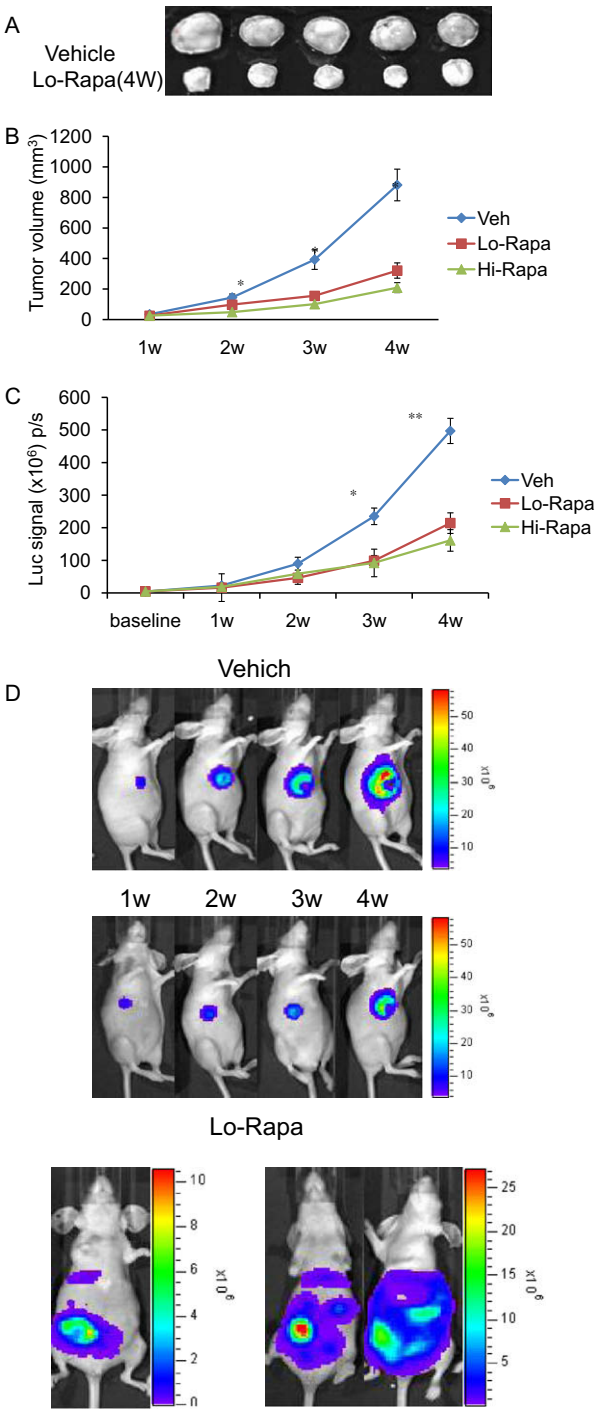


**Fig. 1 – Inhibitory effect of rapamycin on the growth of orthotopic MDA-MB-231 breast cancer over time in the mouse model. Tumour-bearing mice were treated with rapamycin (low dose: 1.5 mg/kg, high dose: 5 mg/kg). Then, tumours were harvested by the end of the 4th week. (A) Representative tumour load ($n = 5$) in low-dose Rapa group versus control. (B) Caliper measurement of tumour growth over 4 weeks in both Lo- and Hi-dose of Rapamycin treatment and the control groups. (C) The effects of both high and low doses of rapamycin on tumour growth over 4 weeks. (D) *In vivo* bioluminescence imaging showing the inhibitory effect of Rapa on tumour growth in the low-dose group over four weeks. (E) High-dose rapamycin promoted metastasis of primary MDA-MB-231 cancer, arrows pointing to the primary tumour sites. Rapa: rapamycin, Hi: high dose, Lo: low dose. *$P < 0.05$, **$P < 0.01$, $n = 5$–6/group.**

antibody (pAkt, 1:1000, Cell Signalling) overnight at 4 °C. After washing with PBST, the membranes were incubated with secondary antibody 1:5000 for 1 h at room temperature and then incubated with detection kit for 1 min (Pierce, USA). The band density was analysed by the software Quantity One (ImageJ, USA). Each experiment was repeated independently. Then

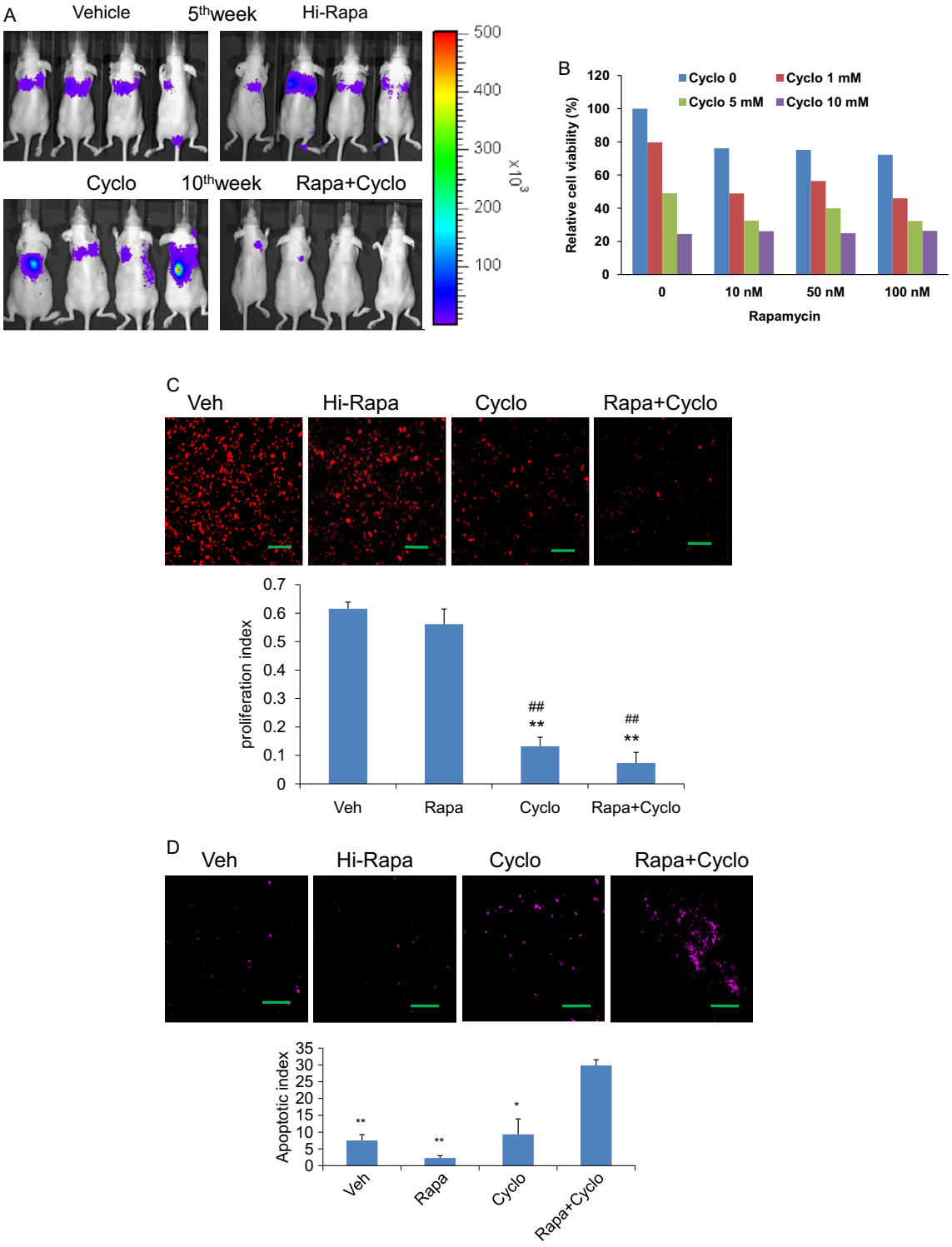


**Fig. 2 – (A) Bioluminescence imaging of lung-metastatic breast cancer cells at 5 weeks (control and Rapa alone group), and 10 weeks (Cyclo alone and combination therapy-treated group) post tumour cell implantation ($2 \times 10^5$ cells by i.v. injection), showing that the effects of rapamycin monotherapy and combination therapy on the lung-metastasis of MDA-MB-231 breast cancer ($n$ = 5/group). (B) The cell viability of MDA-MB-231 at different dosage and combination treatment for 48 h. (C) and (D) show the effect of rapamycin alone and combined with cyclophosphamide on the proliferation and apoptosis of lung-metastatic MDA-MB-231 breast cancer ($n$ = 3–4/group). (C) Ki67 positive cells and proliferation index in different group, scale bar = 100 μm. $^{**}P < 0.01$, versus the control group; $^{\#\#}P < 0.01$, versus Hi-Rapa group. (D) TUNEL-positive cells and apoptotic index in different groups, scale bar 100 μm; $^{*}P < 0.05$, $^{**}P < 0.01$, versus Hi-Rapa + Cyclo group.**

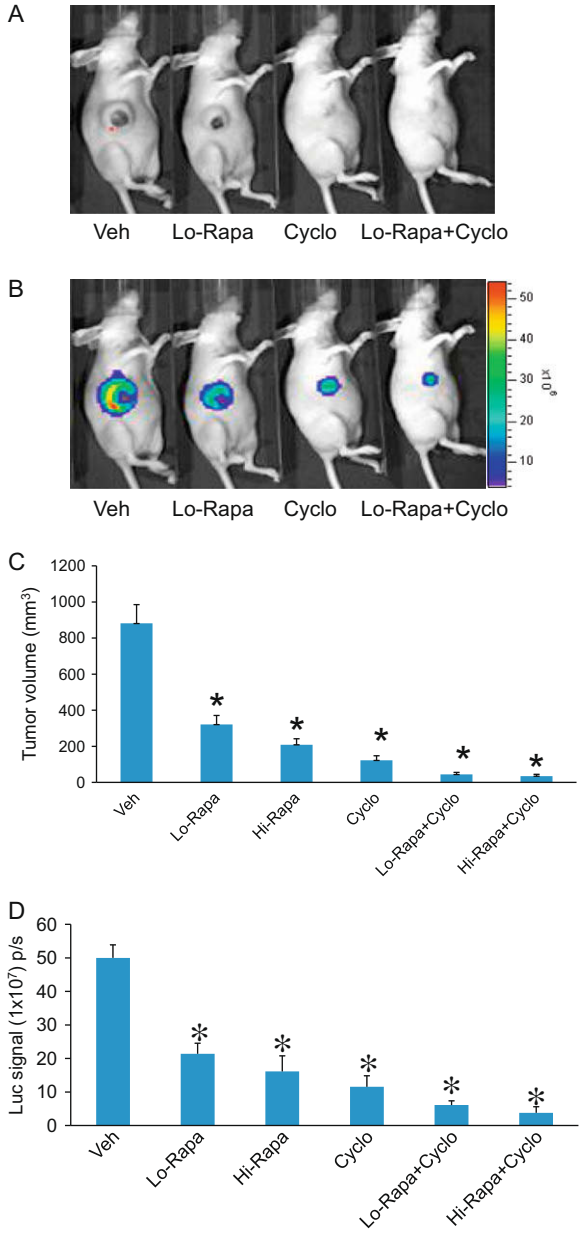


**Fig. 3 – Synergic inhibition of rapamycin and cyclophosphamide on orthotopic mammary MDA-MB-231 cancer ($n$ = 6/group). (A) Grayscale photograph of mice from the control, Lo-Rapa (1.5 mg/kg), Cyclo (150 mg/kg) and Lo-Rapa + Cyclo groups at 4 weeks post cell implantation. (B) Corresponding bioluminescence images of A. (C) Tumour volume measured by caliper in different group. (D) Tumour load measured by bioluminescence imaging in different group. *$P < 0.01$.**

the membranes were stripped with a mild stripping buffer (Pierce, USA) and re-incubated with first antibody AKT 1: 3000 (Cell Signaling, USA).

### 2.8. *Statistical analysis*

Statistical analysis was done using a 2-way ANOVA for multiple groups and an unpaired Student's $t$ test. $P$ values <0.05 were considered statistically significant (GraphPad Prism).

## 3. Results

### 3.1. *Rapamycin alone inhibits the growth of orthotopic breast cancer but promotes its metastasis in vivo*

Previous studies by other laboratories[12] have shown that MDA-MB-231 cell line is resistant to the rapamycin-induced proliferation inhibition *in vitro*. To determine whether MDA-MB-231 cells are resistant to rapamycin *in vivo*, we examined the effects of two different doses of rapamycin, 1.5 mg/kg (Lo-Rapa) and 5 mg/kg (Hi-Rapa), respectively, on tumour growth in nu/nu mice with orthotopic mammary MDA-MB-231 tumour. The drug treatment began on post-implantation day 4. Tumour growth of treated mice was significantly suppressed by rapamycin compared with the control group in the 3rd and 4th weeks (Fig. 1A, $P < 0.01$), but there was no significant difference between the two doses of rapamycin (Fig. 1B and C, $P > 0.05$). All six mice in the Lo-Rapa group and six of seven mice in the Hi-Rapa group responded to rapamycin treatment as measured by caliper and bioluminescence imaging. The volume of tumour, presented as mean ± SEM, reduced from 881.27 ± 103.94 $mm^3$ in the control group to 320.84 ± 49.79 $mm^3$ (63.59% inhibition) in the Lo-Rapa group and 208.74 ± 32.68 $mm^3$ (76.31% inhibition) in the Hi-Rapa group ($P < 0.01$), respectively, in the 4th week after treatment. The intensity of luciferase signal of tumours reached $5.00 \times 10^8$ photon/s in the control group in the 4th week (Fig. 1D). The corresponding readings in the Lo- and Hi-Rapa groups were 57.08% and 67.62% lower ($P < 0.01$), respectively. Therefore, our results showed that MDA-MB-231 cells are sensitive to rapamycin therapy *in vivo*.

Interestingly, from the mice with orthotopic breast cancer, we also found that high dose of rapamycin promoted tumour metastasis (Fig. 1E). The rate of tumour metastasis was 9.9% (1/11) in the control group as metastasis began to appear in bioluminescence imaging in the 4th week. In the Hi-Rapa group, 28.57% of the mice (2/7 mice) developed metastasis, starting in the 3 week, while no mice in the Lo-Rapa group were found to have metastasis ($n$ = 6).

### 3.2. *Rapamycin alone does not inhibit the growth of MDA-MB-231 cancer in the lung*

To assess the influence of an oxygen-rich environment on the response of MDA-MB-231 cell to rapamycin treatment and evaluate the effects of rapamycin on metastasised tumour, we established a lung-metastatic model by injecting MDA-MB-231 cells via the tail veins of mice, and then treated the mice with a high dose of rapamycin. Bioluminescence imaging showed that there was no significant difference between the control and rapamycin-treated groups (Fig. 2A, $P > 0.05$). Rapamycin alone did not inhibit the growth of lung-metastatic MDA-MB-231 cells as we observed significant signals in the lungs by the 5th week. Cyclophosphamide alone also did not inhibit lung metastasis as by the 10th week we can observe luciferase signals in the lungs. The group that received the combination therapy had much weaker signals, even by the 10th week. This observation was consistent with the result of treating MDA-MB-231 with rapamycin *in vitro* (Fig. 2B). In concurrence with this result, there was no

**Table 1 – Bioluminescent imaging intensities and breast cancer sizes ($n$ = 6–11).** Numbers are presented as mean ± SEM.

| Group | Luc signal (photons/s) | Tumour size ($mm^3$) |
|---|---|---|
| Control | $5.0 \times 10^8 \pm 3.9 \times 10^7$ | 881.27 ± 103.94 |
| Low rapamycin | $2.14 \times 10^8 \pm 3.2 \times 10^{7*}$ | 320.84 ± 49.78* |
| High rapamycin | $1.61 \times 10^8 \pm 4.6 \times 10^{7*}$ | 208.74 ± 32.68* |
| Cyclophosphamide | $1.15 \times 10^8 \pm 3.3 \times 10^{7*}$ | 122.17 ± 24.9* |
| Lo-Rapa + Cyclo | $6.11 \times 10^7 \pm 1.2 \times 10^{7*}$ | 44.08 ± 10.99* |
| Hi-Rapa + Cyclo | $3.78 \times 10^7 \pm 1.8 \times 10^{7*}$ | 34.86 ± 9.44* |

* $P < 0.05$ versus control group.

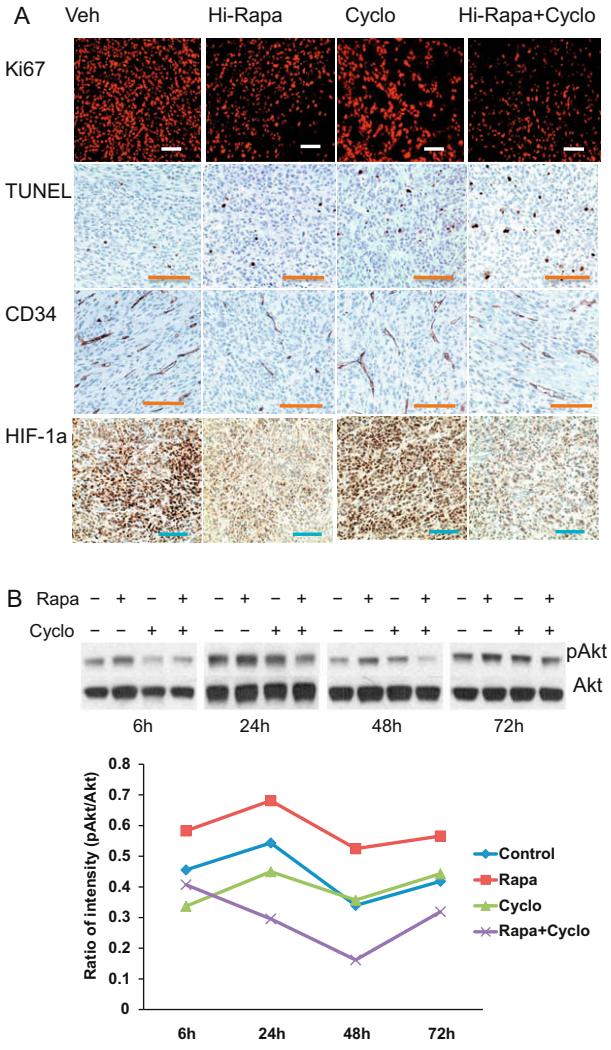


**Fig. 4 – (A) Immunofluorescence and immunohistochemical analysis of orthotopic MDA-MB-231 tumour masses derived from untreated and treated mice. The samples were taken at 4 weeks. Immunostaining showed that Ki67-, CD34- and HIF-1α and TUNEL-positive cells after treatment by rapamycin alone or combined with cyclophosphamide (magnification is 20×, scale bar = 100 μm, $n$ = 3–4/group). (B) The level of phosphorylation and total Akt after drug treatment (Rapa 100 nM, Cyclo 5 mM and both combination) at different time points and ratios.**

**Table 2 – Proliferation and apoptosis index of orthotopic breast cancer ($n$ = 3–4).** Numbers are presented as mean ± SEM.

| Group | Ki67 index (+cells/total cells) | TUNEL index (+cells/per field) |
|---|---|---|
| Control | 0.84 ± 0.02 | 17.05 ± 3.01 |
| High rapamycin | 0.59 ± 0.02** | 31.8 ± 4.54* |
| Cyclophosphamide | 0.62 ± 0.01** | 40.73 ± 6.09* |
| Hi-Rapa + Cyclo | 0.49 ± 0.05** | 52.9 ± 8.85* |

* $P < 0.05$ versus control group.
** $P < 0.01$ versus control group.

**Table 3 – MVD and HIF-1α expression of orthotopic breast cancer ($n$ = 3–4).** Numbers are presented as mean ± SEM.

| Group | MVD ($CD^+$ stain/per field) | HIF-1α score (+cells/per field) |
|---|---|---|
| Control | 180.27 ± 26.73 | 638.56 ± 37.76 |
| High rapamycin | 90.04 ± 24.37* | 280.78 ± 20.38** |
| Cyclophosphamide | 107.58 ± 10.22* | 863.67 ± 7.88*# |
| Hi-Rapa + Cyclo | 102.56 ± 11.61* | 231.22 ± 34.49**$ |

* $P < 0.05$ versus control group.
** $P < 0.01$ versus control group.
# $P < 0.01$ versus Rapa group.
$ $P < 0.01$ versus Cyclo group.

significant difference in ki67 and TUNEL index between Rapa-treated and control mice (Fig. 2C and 2D), implying that the response of lung-metastatic MDA-MB-231 cells to rapamycin is different from that of the orthotopic tumour as they were more resistant to the growth inhibition of rapamycin.

### 3.3. *Inhibition of orthotopic MDA-MB-231 tumour growth by a combination of rapamycin and cyclophosphamide*

To examine the effect of rapamycin plus cyclophosphamide on the growth of MDA-MB-231 breast cancer *in vivo*, we treated tumour-bearing mice with cyclophosphamide in combination with either a high or a low dose of rapamycin. Our data show that the combination therapy has higher efficiency on MDA-MB-231 breast cancer (Fig. 3 and Table 1). The average orthotopic tumour volume was 44.08 $mm^3$ (Lo-Rapa + Cyclo group), 34.86 $mm^3$ (Hi-Rapa + Cyclo group), 122.17 $mm^3$ (Cyclo group), 320.84 $mm^3$ (Lo-Rapa group) and 208.74 $mm^3$ (Hi-Rapa

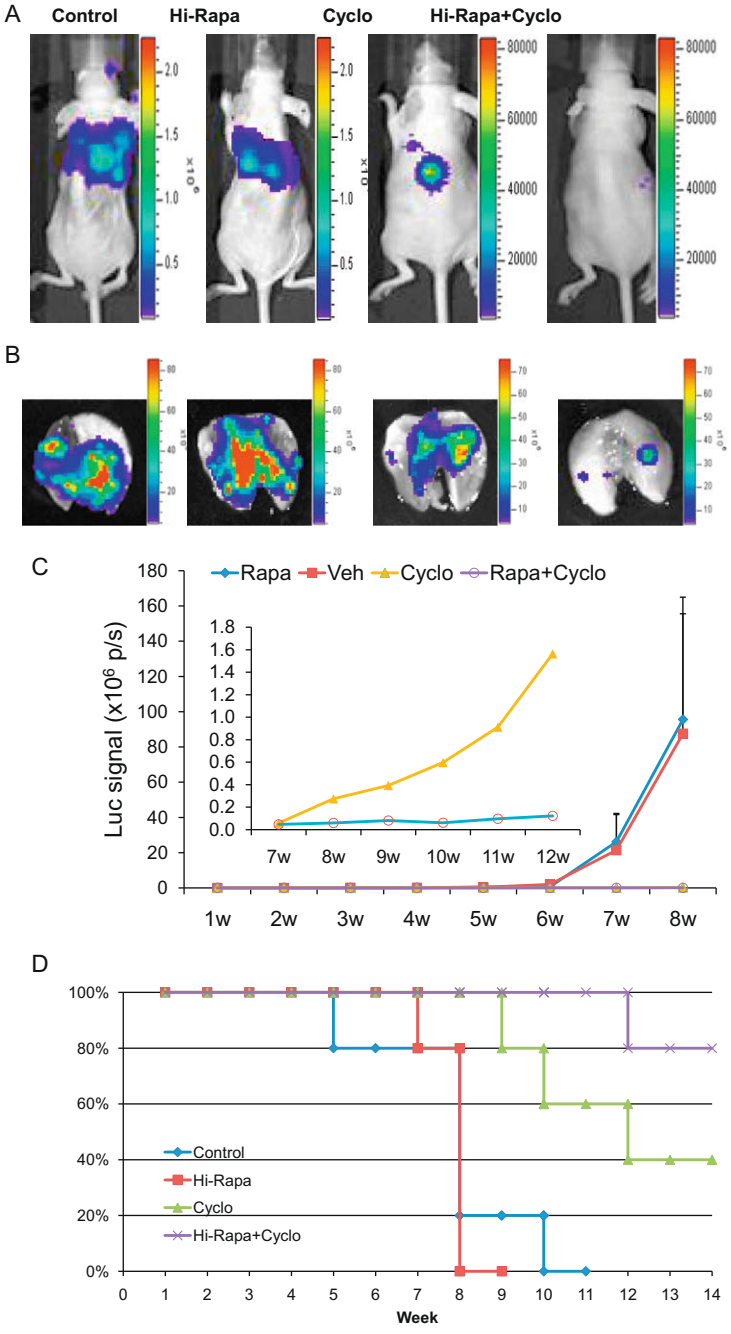


**Fig. 5 – Combination therapy reverses the resistance of MDA-MB-231 cells to rapamycin in mouse lung-metastasis model (*n* = 5/group). A: *In vivo* images taken at the 8th week post tumour cell implantation. (B) At the end of the experiments lungs were harvested for *ex vivo* bioluminescence imaging. Lung images were taken at the 8th week in the control and Rapa groups and at the 14th week in the Cyclo and Rapa + Cyclo groups. (C) Time course of luciferase signal intensity of lung-metastatic tumour for each group. (D) Survival curve of different groups over a 14-week period.**

group) in the 4th week (Table 1). Compared with the Lo-Rapa group, the average tumour mass and luciferase signal intensity of the Lo-Rapa + Cyclo group were 86.26% and 71.42% lower ($P < 0.01$), respectively. Compared with the Hi-Rapa group, the average tumour mass and luciferase signal intensity of the Hi-Rapa + Cyclo group were 83.33% and 84.29% lower ($P < 0.01$), respectively. Compared with the control group, the tumour volume dramatically reduced by 95–96.04% ($P < 0.001$) and luciferase signal decreased 87.69–95.89% in the two combination treatment groups ($P < 0.001$). Tumour growth inhibition appeared earlier in the combination treatment groups (2nd week $P < 0.01$) than those in the rapamycin-alone group (3rd week, $P < 0.05$). There was no significant difference between the two groups that received the combination treatment ($P > 0.05$).

We also performed histology experiments on tumour tissue sections derived from orthotopic xenograft. As shown in Fig. 4A and Tables 2 and 3, treatment with either Rapa or

Cyclo alone led to a decreased Ki67- and an increased TUNEL-positive cells and decreased signals in CD34 staining. The inhibiting rate of proliferation reached 29.76% and 26.19% after Rapa or Cyclo treatment ($P < 0.01$), respectively; indices of apoptosis of both groups were 1.87 and 2.39 times higher than the control group ($P < 0.05$), respectively. MVD of the tumours was 50.05% and 40.32% less for the mice in the Rapa and Cyclo groups than that in the control group ($P < 0.05$), respectively. Combination therapy group had a growth inhibition that was elevated by 20.97% (versus Rapa alone) and 20.96% (versus Cyclo alone); accordingly, apoptosis percentage was raised 66.35% and 23.0%, respectively, indicating that cyclophosphamide can significantly increase the rapamycin-induced effect of apoptosis. However, MVD of tumours did not have significant changes between the groups that received individual or combination treatments ($P > 0.05$). These data suggest that the additive anti-tumour mechanism of rapamycin and cyclophosphamide might be linked to the proliferation inhibition and apoptosis induction while anti-apoptotic effect may be more prominent (Tables 2 and 3).

One of the mechanisms of rapamycin resistance is involved in the feedback activation of Akt through mTOR inhibition.[19,20] To observe this feedback activation phenomenon and examine the effect of cyclophosphamide on the phosphorylated Akt (pAkt), we treated MDA-MB231 cells with rapamycin (100 nM) or/and cyclophosphamide (5 mM) for 6, 24, 48 and 72 h. The results showed that pAkt increased in the rapa alone group at all time points, compared to the control group; but pAkt level did not significantly increase, and even decreased, in Cyclo alone and a combination therapy-treated groups (Fig. 4B). These results demonstrated that rapamycin can persistently induce Akt signalling, while cyclophosphamide inhibits Akt phosphorylation, thereby, breaking the loop of feedback activation Akt inducing by rapamycin inhibition of mTOR.

### 3.4. *The combination regimen reverses the resistance of lung-metastatic breast cancer to rapamycin*

We note that the combination therapy of rapamycin (high-dose) and cyclophosphamide remarkably suppressed the growth of lung-metastatic MDA-MB-231 breast cancer (Fig. 5A and B), although rapamycin alone was not found to have such an effect. This observation is in consistence with the results of the *in vitro* experiment of MDA-MB-231 cell line (Fig. 2A and B). Bioluminescence imaging showed that strong luciferase signals could be detected from the 3rd week in the control and Hi-Rapa groups, from the 7th week in the Cyclo group but only from the 8th week in the combination treatment group in the lung-metastasis model. Luciferase signals of mice that received the combination treatment were obviously lower than those of all the other groups. The signal intensity was more than 1480 times higher in the control group, 1620 times higher in the rapa group than that of the combination group in the 8th week. The average signal intensity of mice treated by Cyclo alone was 4.66 and 12.81 times higher than those of the Hi-Rapa + Cyclo mice in the 8th and 12th weeks, respectively, (Fig. 5C). In addition, survival analysis shows that mice began to die in the 6th week in the control group, 8th week in the Hi-Rapa group, 10th week in the Cyclo group and 13th week in Hi-Rapa + Cyclo group (Fig. 5D). Overall, our results showed that the combination therapy not only inhibited the tumour growth dramatically but also prolonged the survival of the mice that received the combination therapy.

The combination therapy notably inhibited proliferation and induced apoptosis of tumour cells compared with the control and rapamycin groups ($P < 0.01$) (Fig. 2C and D). The proliferation index decreased 86.98% (versus Rapa group $P < 0.01$) and 46.69% (versus Cyclo group), and the apoptotic index increased 11.97 times (versus Rapa group, $P < 0.01$) and 2.2 times (versus Cyclo group, $P < 0.05$). It suggests that rapamycin and cyclophosphamide combination may reverse the resistance of lung-metastatic MDA-MB-231 to rapamycin in an oxygen- and vasculature-rich environment.

### 3.5. *Influence of HIF-1α level on the anti-tumour effect of rapamycin*

HIF-1α is an oxygen-sensitive transcription factor regulated by the mTOR pathway. To evaluate the role of HIF-1α responsible in Rapa- or Cyclo-therapy, we measured the expression of HIF-1α in orthotopic MDA-MB-231 breast cancer (Table 3). The expression of HIF-1α was markedly down-regulated by rapamycin, but up-regulated by cyclophosphamide, which is consistent with the results reported by other researchers.[21] HIF-1α up-regulation promotes the secretion of proangiogenic cytokines such as VEGF and FGF, leading to angiogenesis in tumour tissue. In our experiments, we found that HIF-1α and MVD were down-regulated after the rapamycin treatment. Linear regression analysis indicated that there was a positive correlation between HIF-1α scores and MVD in the rapamycin treatment group in orthotopic MDA-MB-231 breast cancer ($r = 0.996$). The mechanism in the destruction of tumour vasculature might be associated with HIF-1α down-regulation by rapamycin; while the reduction of MVD caused by cyclophosphamide might be HIF-1α-independent. Furthermore, the combination regimen did not reduce MVD and HIF-1α when compared with Rapa-treated mice, a phenomenon that may be related to the fact that cyclophosphamide increases the expression of HIF-1α in the tumour cells.

In lung-metastatic tumours, no specific signal of HIF-1α was detected at the 8th week after tumour cell injection in all groups, implying the level of HIF-1α in lung-metastatic MDA-MB-231 cancer was very low or undetectable. The mean MVD was $113.11 \pm 27.71$ (mean ± SEM) in the control group, and $86.11 \pm 3.82$ in the Rapa-treated group, respectively. It showed a decline of MVD in the Rapa-treated group, but there was no statistical difference between this group and the control group, implying that there was a HIF-1α-independent mechanism involved in the angiogenesis of lung-metastatic MDA-MB-231 breast cancer in our model. In orthotopic mammary tumour rapamycin's down-regulation of high expression of HIF-1α was accompanied by tumour growth inhibition, while lung-metastatic tumour with low level of HIF-1α did not respond to rapamycin treatment. This result suggested that HIF-1α down-regulation might play an important role in Rapa-therapy alone, but might not in Rapa-Cyclo combination.

## 4. Discussion and conclusions

The establishment of mouse models with luciferase-transfected MDA-MB-231 breast cancer cells in combination with bioluminescent imaging provides a method for rapid, non-invasive and quantitative analysis of tumour biomass and metastasis. Using this preclinical model we demonstrate that (1) Orthotopic MDA-MB-231 breast cancer is highly sensitive to rapamycin therapy, as rapamycin decreases proliferation, increases apoptosis of cancer cells and reduces tumour vascularity. (2) The same cancer cells that metastasised to the lungs appeared to be resistant to rapamycin monotherapy, similar to their response to rapamycin *in vitro*. (3) HIF-1α down-regulation might be a mechanism of the anti-tumour effect of rapamycin on orthotopic MDA-MB-231 breast cancer. (4) The combination of rapamycin with cyclophosphamide has a stronger inhibiting effect on MDA-MB-231 breast cancer growth in mouse and reverses the rapamycin resistance of lung-metastatic MDA-MB-231 cancer. (5) High-dosage (5 mg/kg) of rapamycin alone promoted the metastasis of MDA-MB-231 breast cancer in orthotopic model, which according to the best of our knowledge is the first *in vivo* experimental evidence of such effect of rapamycin.

The human MDA-MB-231 cell line is resistant to rapamycin treatment *in vitro* because it has some common features that contribute to its rapamycin-resistant molecular mechanism, including low activity of Akt, high level of phospholipase D (PLD),[22] negative oestrogen receptor, and low expression of Her2. However, as shown in our study, the response of MDA-MB-231 cell line to rapamycin *in vivo* was more complicated: the tumour growth was significantly inhibited under the mammary fat pads but not in the lungs, indicating that the microenvironmental difference between the mammary fat pads and lungs may influence the response of tumour cells to rapamycin therapy.

Cancer cells commonly experience hypoxia due to their fast growth. Hypoxia, in turn, leads to HIF-1α up-regulation, which facilitates oxygen delivery to cancer cells and helps them adapt to oxygen deprivation by activating genes that control glucose uptake, metabolism, angiogenesis, erythropoiesis, cell proliferation and apoptosis. Therefore, under hypoxic conditions, HIF-1α plays a facilitating role in tumour progression and its level may determine the severity of cancer progression. In many types of cells, PI3 kinase/Akt signalling regulates HIF activity in an mTOR-dependent manner,[23] and HIF-1α is also known to be sensitive to rapamycin treatment.[24] In our breast cancer orthotopic models, MDA-MB-231 cells grew in mammary fat pad where there is a relatively lower concentration of oxygen and less vasculature. The high expression of HIF-1α in these cancer sites was reduced by rapamycin treatment, indicating that a decrease in HIF-1α level was accompanied by a significant inhibition of tumour growth.

Unlike mammary fat pad, the environment in the lungs is rich in oxygen and microvasculature, which may fulfill the metabolic requirements of tumour growth. This oxygen-rich environment is similar to *in vitro* cell culture, where it was found that the cell line is resistant to rapamycin. An environment rich in oxygen inhibits the expression and promotes rapid degradation of HIF-1α.[25] Our immunohistochemistry results show that HIF-1α is at an undetectable level in the metastatic cancer region in the lungs at 8 weeks after cancer cell implantation in the metastastic model. Since HIF-1α expression is lower in the lungs than in the mammary fat pad, rapamycin, which suppresses cancer cell growth partly through the inhibition of HIF-1α, would have a less therapeutic effect in the lungs (an oxygen-rich environment) than in the mammary environment. A previous study of kidney cancer by Thomas and colleagues suggested that HIF-1α level determines sensitivity of renal cancer cells to inhibition of mTOR (CCI-779).[13] When the level of VHL protein in the kidney, which promotes the HIF-1α by encoding E3 ligase, is reduced by VHL shRNA, levels of HIF-1α and HIF-2α increase in the kidney cancer cells, resulting in a more rapid proliferation of the cancer cells and an increase in the sensitivity of these cells to CCI-779. Rapamycin monotherapy failed to inhibit the growth of lung-metastatic MDA-MB-231 cancer. On one hand, the change of oxygen-microenvironment can alter the level of HIF-1α, which influences the response of breast cancer to rapamycin treatment. On the other hand, oxygen and nutrient can modulate mTOR signalling, which, in turn, likely affects the effect of rapamycin. In addition, it is possible that there are other mechanisms by which tumour cells rapidly proliferate under vessel-rich conditions when HIF-1α is inhibited or knocked out. Blouw and colleagues also found that the growth of HIF-1α knockout astrocytoma is faster in the vascular-rich brain parenchyma than in the vessel-poor subcutaneous (s.c.) environment.[26] Therefore, the resistance mechanism to rapamycin therapy is very complex and warrants further investigation.

As a single agent, rapamycin's efficacy is limited because it promotes Akt signalling by a feedback activation of the IRS-PI3K pathway and shifts the equilibrium towards the mTOR-GßL-rictor complex.[20] We combined rapamycin with cyclophosphamide to treat MDA-MB-231 breast cancer and demonstrated that the combination not only dramatically suppressed both primary and metastatic tumour growth and prevented tumour metastasis, but also reversed the resistance of lung-metastatic cancer to rapamycin monotherapy and prolonged the survival of the tumour-bearing mice.

In our study the mice that received combination therapy had much less tumour size and Luc-signal intensity than those in the control group and the groups received either rapamycin or cyclophosphamide alone. This much increased tumour inhibitor effect of rapamycin and cyclophosphamide may be due to the reason that the two drugs primarily enhance each other in inhibiting proliferation and inducing apoptosis. This additive effect was observed in both orthotopic and lung-metastatic models and was more prominent in the latter model, probably because the rich vasculature of the lungs enhances drug delivery. Our data also showed that the combination treatment did not have an increased anti-angiogenesis effect compared with monotherapy, probably for the reason that cyclophosphamide elevated the expression of HIF-1α in tumour cells. Therefore, a decrease of MVD might not contribute to the anti-cancer effect in the groups that received the combination therapy. Previous studies demonstrated that RAD001, a mTOR inhibitor, can make cancer cells more sensitive to the effect of DNA-

damaging drugs through p21 translation.[15] A recent study demonstrated that the combination of letrozole with cyclophosphamide significantly reduced both PI3K/pAKT and phospho-mTOR expression.[27] In the study, no changes in pAKT level were observed in patients treated with letrozole only, whereas a significant decrease of pAKT level was observed in the group that received combined treatment. The interaction between rapamycin and cyclophosphamide might also involve p21 translation and AKT phosphorysation. In our study, we found that rapamycin can persistently induce Akt activation, while cyclophosphamide can prevent this feedback activation of Akt. This might be one mechanism by which the combination strategy enhances the anti-tumour effect of rapamycin. Guba and colleagues proposed that it is critical to control the dosage of rapamycin to achieve optimal antiangiogenic effect for cancer treatment.[28] They found that higher levels (4.5 mg/kg/3 d bolus) of rapamycin did not improve its inhibitory effect on CT-26 colon adenocarcinoma. When we examined rapamycin's growth inhibitory effect at low (1.5 mg/kg) and high dose (5 mg/kg) on orthotopic MDA-MB-231 breast cancer, we found that high dose did not significantly improve anti-tumour response, which was consistent with Guba's study.[28] Furthermore, as it was shown in our *in vivo* data, high dosage of rapamycin had the side-effect of promoting migration of MDA-MB-231 cells to form a new tumour colony. Therefore, in addition to identifying the drug sensitivity, we also need to determine the optimal dosage of rapamycin as a breast cancer therapy.

Beside intrinsic properties of tumour cells, external microenvironment of tumour growth might induce changes of some intracellular proteins such as HIF-1$\alpha$ in mammary and lung environment, leading to an alteration in drug resistance. The combination of rapamycin with cyclophosphamide had a stronger anti-tumour effect because they mutually enhance each other by promoting apoptosis and inhibiting tumour cell proliferation. It is likely that the combination therapy has a 'doubling' effect in modulating the PI3k/Akt and mTOR pathway, although more studies are needed to further elucidate the detailed mechanisms. This combination regimen may offer a promising therapy for breast cancer, especially for TN and rapamycin-resistant types of breast cancer.

As an *in vivo* imaging technique, bioluminescent imaging is quantitative and highly sensitive, making it well suited to study tumour development and metastasis.[29] The system we used in this work, however, can only acquire 2D planar images of the animals. It cannot pinpoint the location of the luciferase-transfected cells and the readout is affected by many factors like light attenuation and scattering in tissue.[30] Therefore, careful design of experiments and analysis of the quantitative data are required. Despite these limitations, bioluminescent imaging is well suited for oncology studies for its high throughput and capability to monitor dynamic processes, especially in monitoring metastasis, in which it is often not known *a priori* the location of tumour migration. In combination with other imaging modalities like MRI and micro PET/CT, one can acquire both anatomic and dynamic information, thus leading to a better understanding of tumourigenesis and its response to treatment.

## Conflict of interest statement

None declared.

## Acknowledgements

We thank X. Yuan of Department of Medicine, Beth Israel Deaconess Medical Center for his technical help. The work of Q. Zeng and X. Xu is supported by a program grant awarded to the Optical Imaging Lab, Department of Radiology, Brigham and Women's Hospital. The work of K. Cui and S.T.C. Wong was supported by the Functional and Molecular Imaging Center Program of Brigham and Women's Hospital.

## REFERENCES

1. Kassam F, Enright K, Dent R, et al. Survival outcomes for patients with metastatic triple-negative breast cancer: implications for clinical practice and trial design. *Clin Breast Cancer* 2009;**9**(1):29–33.
2. Irvin WJJ, Carey LA. What is triple-negative breast cancer? *Eur J Cancer* 2008;**44**(18):2799–805.
3. Stockmans G, Deraedt K, Wildiers H, Moerman P, Paridaens R. Triple-negative breast cancer. *Curr Opin Oncol* 2008;**20**(6):614–20.
4. Altundag K, Harputluoglu H, Aksoy S, Gullu IH. Potential chemotherapy options in the triple negative subtype of breast cancer. *J Clin Oncol* 2007;**25**(10):1294–5 [author reply 1295–6].
5. Rakha EA, El-Sayed ME, Green AR, et al. Prognostic markers in triple-negative breast cancer. *Cancer* 2007;**109**(1):25–32.
6. Strimpakos AS, Karapanagiotou EM, Saif MW, Syrigos KN. The role of mTOR in the management of solid tumors: an overview. *Cancer Treat Rev* 2009;**35**(2):148–59.
7. Cui X, Zhang P, Deng W, et al. Insulin-like growth factor-I inhibits progesterone receptor expression in breast cancer cells via the phosphatidylinositol 3-kinase/Akt/mammalian target of rapamycin pathway: progesterone receptor as a potential indicator of growth factor activity in breast cancer. *Mol Endocrinol* 2003;**17**(4):575–88.
8. Chan S, Scheulen ME, Johnston S, et al. Phase II study of temsirolimus (CCI-779), a novel inhibitor of mTOR, in heavily pretreated patients with locally advanced or metastatic breast cancer. *J Clin Oncol* 2005;**23**(23):5314–22.
9. Atkins MB, Hidalgo M, Stadler WM, et al. Randomized phase II study of multiple dose levels of CCI-779, a novel mammalian target of rapamycin kinase inhibitor, in patients with advanced refractory renal cell carcinoma. *J Clin Oncol* 2004;**22**(5):909–18.
10. Dancey JE. Therapeutic targets: MTOR and related pathways. *Cancer Biol Ther* 2006;**5**(9):1065–73.
11. Svirshchevskaya EV, Mariotti J, Wright MH, et al. Rapamycin delays growth of Wnt-1 tumors in spite of suppression of host immunity. *BMC Cancer* 2008;**8**:176.
12. Noh WC, Mondesire WH, Peng J, et al. Determinants of rapamycin sensitivity in breast cancer cells. *Clin Cancer Res* 2004;**10**(3):1013–23.
13. Thomas GV, Tran C, Mellinghoff IK, et al. Hypoxia-inducible factor determines sensitivity to inhibitors of mTOR in kidney cancer. *Nat Med* 2006;**12**(1):122–7.

14. Mondesire WH, Jian W, Zhang H, et al. Targeting mammalian target of rapamycin synergistically enhances chemotherapy-induced cytotoxicity in breast cancer cells. *Clin Cancer Res* 2004;**10**(20):7031–42.
15. Beuvink I, Boulay A, Fumagalli S, et al. The mTOR inhibitor RAD001 sensitizes tumor cells to DNA-damaged induced apoptosis through inhibition of p21 translation. *Cell* 2005;**120**(6):747–59.
16. Hengstler JG, Hengst A, Fuchs J, et al. Induction of DNA crosslinks and DNA strand lesions by cyclophosphamide after activation by cytochrome P450 2B1. *Mutat Res* 1997;**373**(2):215–23.
17. Cejka D, Preusser M, Fuereder T, et al. mTOR inhibition sensitizes gastric cancer to alkylating chemotherapy in vivo. *Anticancer Res* 2008;**28**(6A):3801–8.
18. Svagzdys S, Lesauskaite V, Pavalkis D, et al. Microvessel density as new prognostic marker after radiotherapy in rectal cancer. *BMC Cancer* 2009;**9**:95.
19. Garber K. Targeting mTOR: something old, something new. *J Natl Cancer Inst* 2009;**101**(5):288–90.
20. Wan X, Harkavy B, Shen N, Grohar P, Helman LJ. Rapamycin induces feedback activation of Akt signaling through an IGF-1R-dependent mechanism. *Oncogene* 2007;**26**(13):1932–40.
21. Viola RJ, Provenzale JM, Li F, et al. In vivo bioluminescence imaging monitoring of hypoxia-inducible factor 1alpha, a promoter that protects cells, in response to chemotherapy. *AJR Am J Roentgenol* 2008;**191**(6):1779–84.
22. Chen Y, Zheng Y, Foster DA. Phospholipase D confers rapamycin resistance in human breast cancer cells. *Oncogene* 2003;**22**(25):3937–42.
23. Rankin EB, Giaccia AJ. The role of hypoxia-inducible factors in tumorigenesis. *Cell Death Differ* 2008;**15**(4):678–85.
24. Toschi A, Lee E, Gadir N, Ohh M, Foster DA. Differential dependence of hypoxia-inducible factors 1 alpha and 2 alpha on mTORC1 and mTORC2. *J Biol Chem* 2008;**283**(50):34495–9.
25. Salceda S, Caro J. Hypoxia-inducible factor 1alpha (HIF-1alpha) protein is rapidly degraded by the ubiquitin-proteasome system under normoxic conditions. Its stabilization by hypoxia depends on redox-induced changes. *J Biol Chem* 1997;**272**(36):22642–7.
26. Blouw B, Song H, Tihan T, et al. The hypoxic response of tumors is dependent on their microenvironment. *Cancer Cell* 2003;**4**(2):133–46.
27. Generali D, Fox SB, Brizzi MP, et al. Down-regulation of phosphatidylinositol 3′-kinase/AKT/molecular target of rapamycin metabolic pathway by primary letrozole-based therapy in human breast cancer. *Clin Cancer Res* 2008;**14**(9):2673–80.
28. Guba M, Koehl GE, Neppl E, et al. Dosing of rapamycin is critical to achieve an optimal antiangiogenic effect against cancer. *Transpl Int* 2005;**18**(1):89–94.
29. Jenkins DE, Hornig YS, Oei Y, Dusich J, Purchio T. Bioluminescent human breast cancer cell lines that permit rapid and sensitive in vivo detection of mammary tumors and multiple metastases in immune deficient mice. *Breast Cancer Res* 2005;**7**(4):R444–54.
30. Cui K, Xu X, Zhao H, Wong ST. A quantitative study of factors affecting in vivo bioluminescence imaging. *Luminescence* 2008;**23**(5):292–5.